REU Project 2019
1D Seismic Isolation System

Author
Maura Shea

Mentor
Conor Mow-Lowry

UNIVERSITY OF BIRMINGHAM

UF UNIVERSITY of FLORIDA

WELLESLEY COLLEGE

31 July 2019

Contents

1 Introduction

Einstein first discussed gravitational waves in his Theory of General Relativity in 1916, and further developed the theory in his 1918 paper "On Gravitational Waves."[1] Nearly one hundred years after his prediction, the first gravitational waves from a merging binary black hole system were detected by LIGO (Laser Interferometer Gravitational-Wave Observatory) on September 14, 2015.[2] Since then, LIGO has also detected a binary neutron star merger. As sophisticated and complex as LIGO's current design is, there is always room for improvement in scientific instruments.

1.1 6D Project

The 6D Project is, in its simplest form, using interferometers to seismically isolate mirrors, with the ultimate goal of increasing sensitivity for LIGO observations in low frequencies. The 6 dimensions are X, Y and Z directions, and corresponding tilts. All six degrees are necessary know the exact position of the entire test mass in LIGO, and be able to control its location.

While LIGO already has excellent sensors for higher frequencies, the 6D project improves on LIGO at low frequencies, particularly in the RX and RY tilt dimensions. The 6D system (shown in Figure 1) improves low frequency measurements because it lowers the resonant frequency of the system. While data can be used from below the system's resonant frequency, the signal to noise ratio is poor. Lowering the resonant frequency of the system therefore increases the SNR at lower frequencies, down to the new resonant frequency.

In the next generation of LIGO, there will be many scientific enhancements, both from 6D project and other improvements, such as [3]:

- Detection of stellar-mass black hole mergers out to a redshift of $z \approx 6$.
- Sensitive to intermediate-mass black holes up to 2000 solar masses.
- 18x higher detection rate of BH mergers than LIGO.
- 2x better mass constraint.
- Improved localization of binary neutron stars.

1.2 1D Project

The 1D project is a simpler subset of the 6D project. In the 1D project, the focus is on actively monitoring and controlling motion in one dimension - the vertical dimension, with no tilt. This simplified version still has very low noise - Figure 2, shows that the 1D project would perform well at low frequency, with low noise, but at higher frequency the noise does not meet the requirements. By including all six dimensions, the noise level drops well below the required noise for all frequencies.

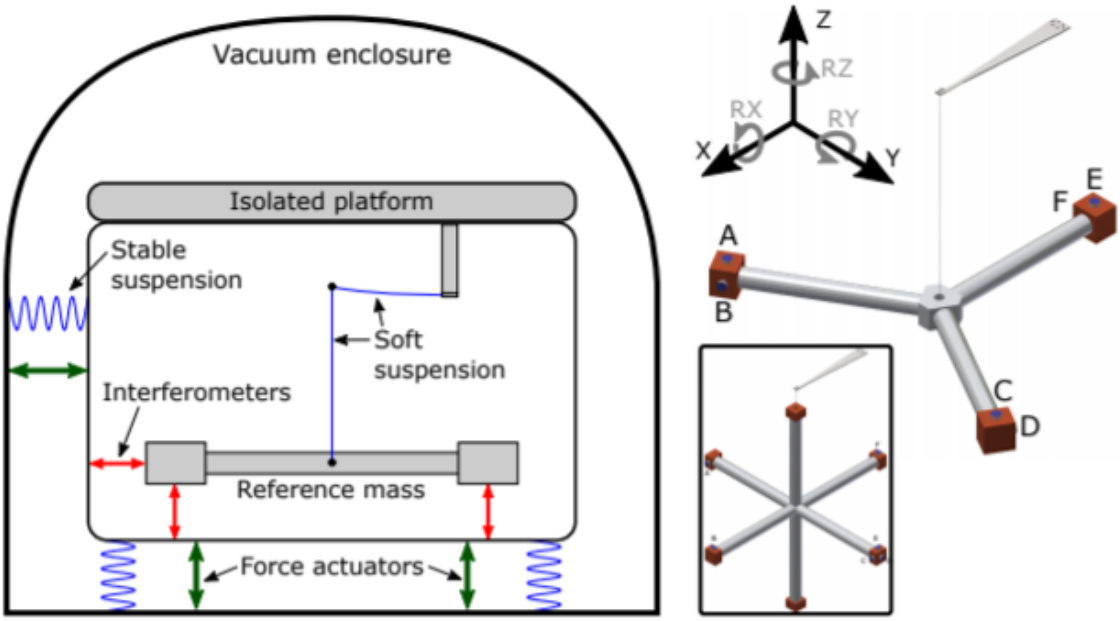

Figure 1: Diagram of the 6D System. A 2-d representation of the isolation architecture (left) and a design concept for the reference mass and suspension (right). Letters indicate interferometric sensing locations. Inset right: an alternative configuration with equal moments of inertia in the three principal axes that reduces Newtonian noise in RX and RY at the expense of size and complexity. Figure and Caption adapted from [4].

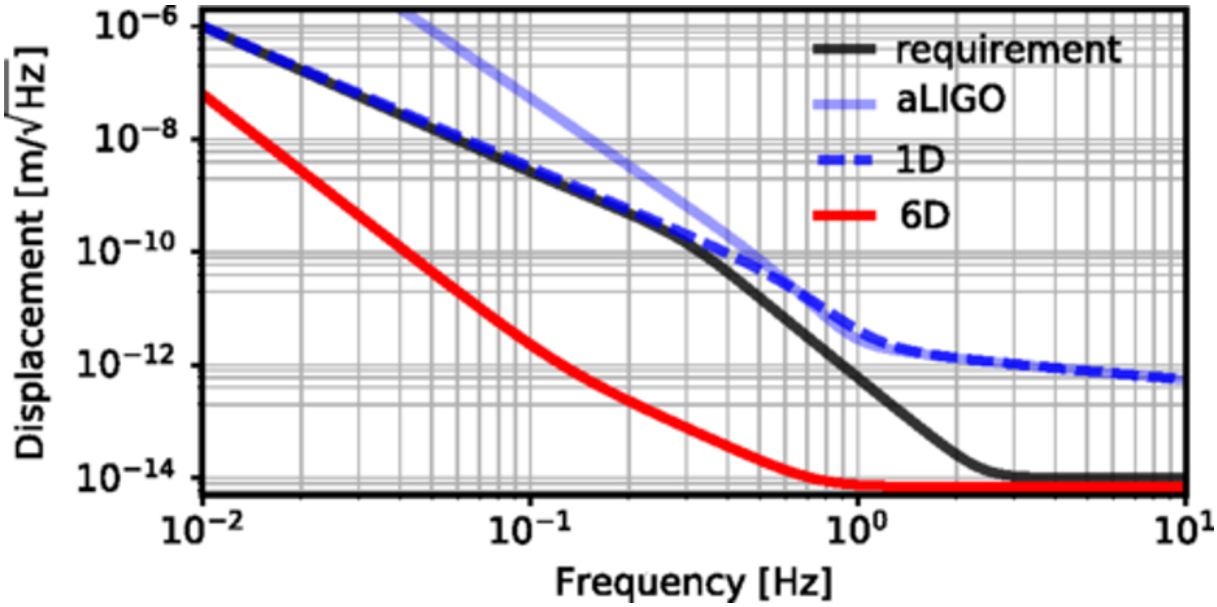

Figure 2: 6D Noise Predictions. The current inertial sensor noise for aLIGO is shown by the light blue line, and the requirement for LIGO-LF is shown by the black line. Custom tiltmeters can be used to improve aLIGO sensor noise below 0.5 Hz (blue dashed line). This 1D component is the focus of this paper's project. A novel 6D seismometer (red line) can surpass the requirement in the entire band. Figure and caption adapted from [3].

The focus of my project this summer was setting up the 1D system and calibrating the components of the 1D system. Once the system was calibrated, we designed and implemented a control system to be able to actively suppress the ground motion via a platform controlled by piezos. We were able to actively control the platform based on a control from an L4C, reaching a noise level near to that of the instrument noise of the L4C.

2 System Setup

The 1D system has many components. The system essentially consists of physical instruments: geophone siesmometers to measure ground motion, a platform on which the siesmometers sit, and piezos to move the platform to cancel out ground motion, shown in Figure 3.

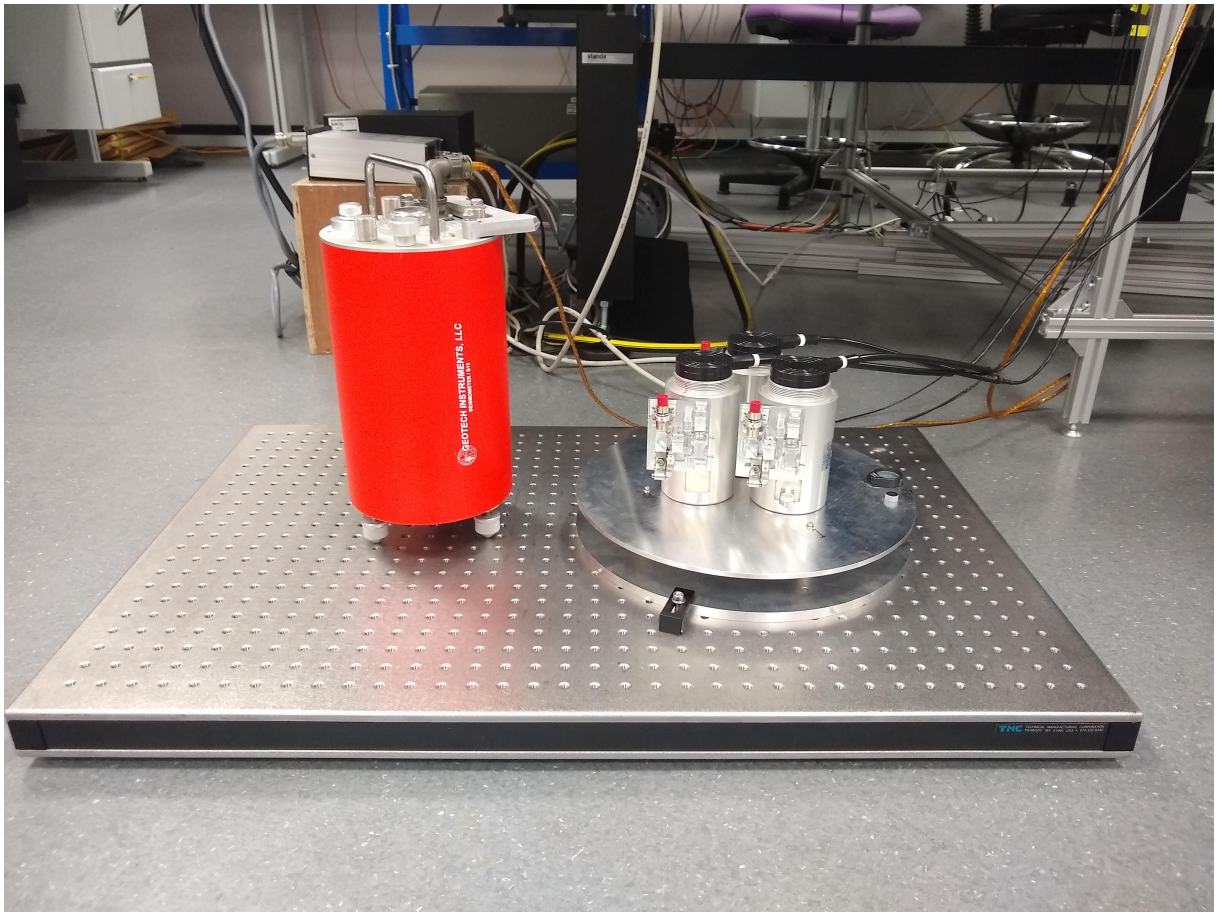

Figure 3: The setup of the physical instruments of the 1D system. The three geophones on the platform are the L4Cs, and the red geophone next to the platform is the S-13. The platform is actuated on by three piezos.

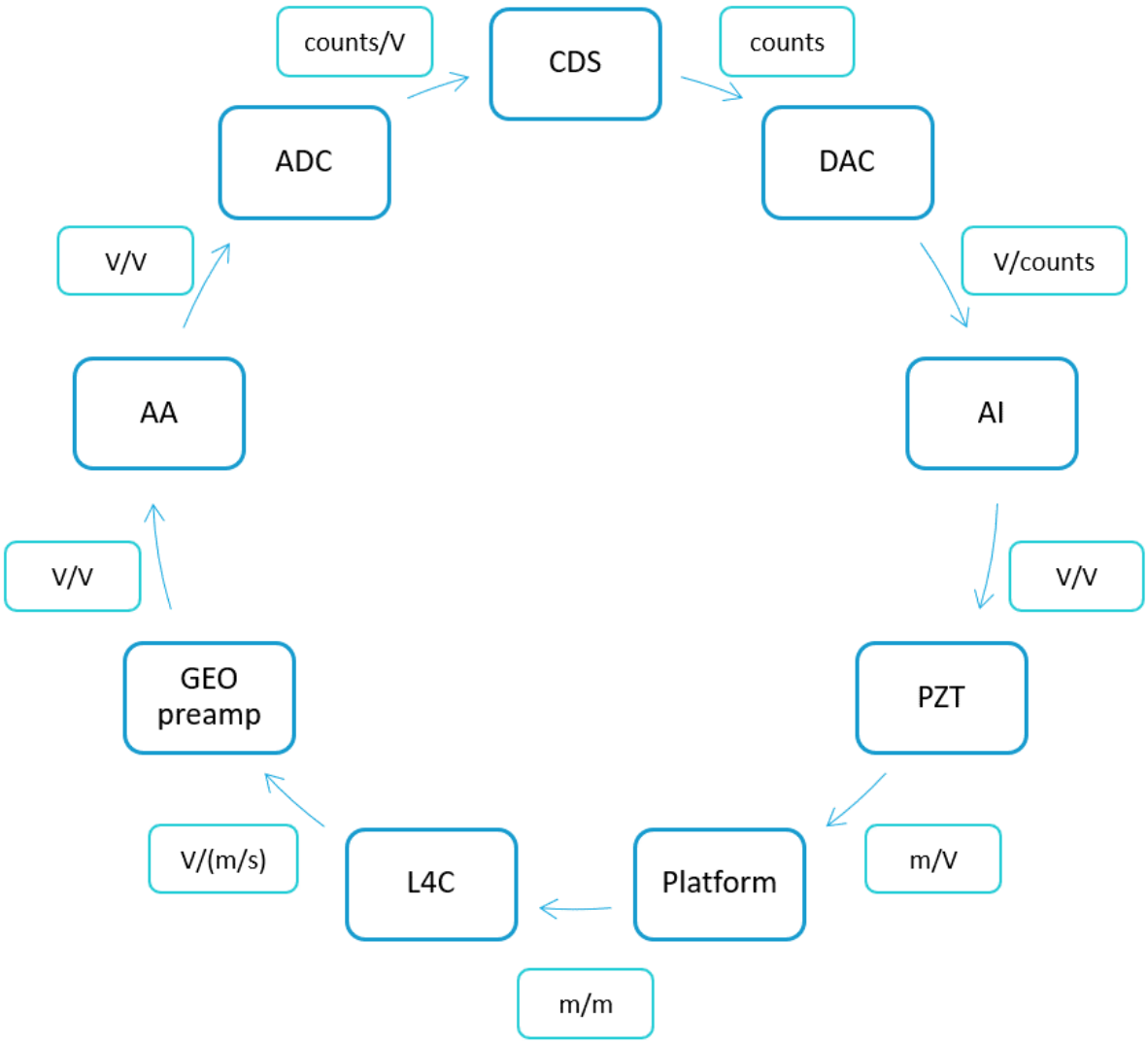

Figure 4: A diagram of how all the components in the system fit together. Output untis are shown; numerical values of the calibrations are discussed in Section 2.2.

2.1 Components

This section details each component of the system. The cycle of the system is diagramed in Figure 4.

CDS
Acronym for Control and Data System. CDS is the computer system we use to measure and record our data. Has a sample rate of 2^{16} samples per second.

Digital to Analog Converter (DAC)
Converts the digital signal from CDS to an analog signal.

Anti-Imaging Filters (AI) and Anti-Aliasing Filters (AA)
These filters account for difference between a model's sampling rate and CDS's sampling rate. A difference in sampling rate can cause a high frequency sine wave appear to be a lower frequency sine wave. The AA filter removes the mirrored high frequency signal that has gotten mirrored down to lower frequency. Additionally, when reversing this process, low frequency signals end up with higher frequency harmonics, which the AI filter removes.

Piezos
The actuators that move the platform. All three piezos receive the same analog signal of volts, which is then translated to physical vertical motion. The specific model we are using is PA 16/14, B202-00.

Platform
A platform that rests on the three piezos, and upon which the geophones sit. This is the platform that will be actively controlled to minimize the motion of the geophones relative to the ground.

L4Cs and S-13
The L4Cs and S-13 are geophones. These seismic instruments measure the velocity difference between an internal mass suspended on a spring and the outer casing of the instrument. They output a voltage that can then be measured by the rest of the system.

Geophone Pre-amplifier
Amplifies the signal received by the L4C.

Analog to Digital Converter (ADC)
Converts the analog signal back into a digital signal readable by CDS.

2.2 System Calibration

In order to be able to accurately quantify the noise from our system, we first had to obtain the calibration factors for each component of the system. In some cases, the calibration factor is very easy - for the Anti-Imaging and Anti-Aliasing Filters, we trust the provided value of $1\left[\frac{V}{V}\right]$. Similarly with the Platform, the conversion is just $1\left[\frac{m}{m}\right]$. For the rest of the components, we had to determine or confirm the calibration factors. The results of the calibration factors are summarized in Table 1.

Component	**Calibration**	
DAC	$\frac{10}{32768}$	$\left[\frac{V}{counts}\right]$
AI	≈ 1	$\left[\frac{V}{V}\right]$
Piezo	0.98×10^{-7}	$\left[\frac{m}{V}\right]$
Platform	≈ 1	$\left[\frac{m}{m}\right]$
L4C	$276.8 \times 2\pi f$	$\left[\frac{V}{m/s}\right]$
Pre-amplifier	200 or 400	$\left[\frac{V}{V}\right]$
AA	≈ 1	$\left[\frac{V}{V}\right]$
ADC	$\frac{32768}{20}$	$\left[\frac{counts}{V}\right]$

Table 1: Summary of calibration factors for closed loop system.

2.2.1 DAC and ADC Calibration

In order to calibrate the DAC and ADC components, we injected a signal into the system with a signal generator at a frequency of 10 Hz, and amplitude of 3 V peak to peak. We then measured the signal with CDS, which yielded an output of $\frac{32768}{20}\left[\frac{counts}{volt}\right]$ for the ADC, and $\frac{10}{32768}\left[\frac{volts}{count}\right]$for the DAC.

2.2.2 Geophone Calibration

To calibrate the L4Cs and S-13, we needed to determine the resonant frequency and quality factor for each device. These values can then be used to create filters in later steps. In order to measure the resonant frequency and quality factor, we needed to measure the ringdown of the L4C's internal mass oscillations. To get only a response of internal oscillations (and not, say, oscillations from the table), we gently picked up the L4C and set it back down. We repeated this process three times for each L4C. We then used the MATLAB script 'ringdownPlot' to fit the ringdown and get measurements for the resonant frequencies and quality factors (one sample of the ringdown plots is shown in Figure 5). The data is recorded in Table 2.

However, after frequently moving the L4Cs around and rearranging the system, we wanted to re-measure the ringdowns to have the most accurate measurement possible. This time, to excite the platform we firmly pressed a thumb into the breadboard and then lifted it. The values for the resonant frequencies and Q factors are very similar to what they were measured to be before. The final results are shown in Table 3.

L4C	**Resonant Frequency**	**Quality Factor**
365 Test 1	1.26	2.08
365 Test 2	1.26	2.09
365 Test 3	1.26	2.08
364 Test 1	1.05	1.64
364 Test 2	1.06	1.65
364 Test 3	1.05	1.66
362 Test 1	1.34	2.24
362 Test 2	1.33	2.28
362 Test 3	1.34	2.24

Table 2: The original ringdown measurements.

Geophone	**Resonant Frequency**	**Quality Factor**
S-13	1.02	7.28
L4C 365	1.27	2.15
L4C 364	1.11	1.66
L4C 362	1.36	2.29

Table 3: The final ringdown measurements used in calibration. The measurements are reasonably consistent with original measurements. Also, the temperature in the room was very different between the two measurements, so some fluctuations in the measurement was expected.

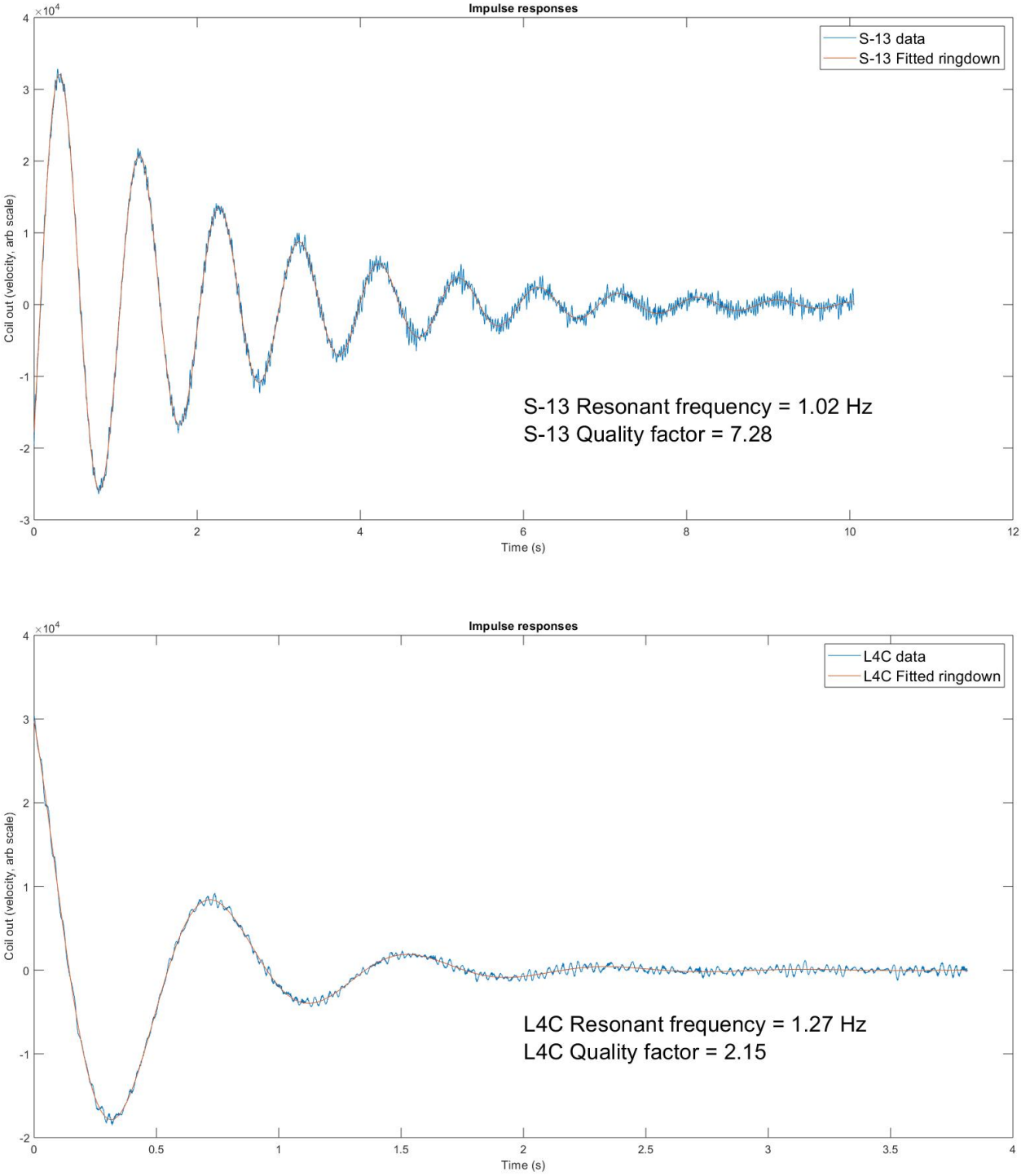

Figure 5: An example of fitting the ringdown of a geophone. Top: The ringdown of the S-13. Bottom: The ringdown of L4C #365.

2.2.3 GEO Pre-amplifier Gain

In order to measure the gain of the pre-amplifier, we connected a signal generator to CDS and the pre-amp, and sent a signal of 0.05 V peak to peak at a frequency of 120 Hz. We connected the pre-amp to CDS, and measured the input and output signals. The amplitude of the input signal was 40 counts. For the monitor output, the output signal was 2000 counts, resulting in a gain of 50. For the differential output, the signal was 4000 counts, resulting in a gain of 100.

Later, the gain of the pre-amplifier was increased from 100 (differential output) to 400 (differential output). To verify this, we connected a signal generator to the pre-amp and applied 10 mV peak to peak to the pre-amp at a frequency of 120 Hz and measured the output with CDS.

2.2.4 Piezo Calibration

To determine the calibration for the piezos, we measured the transfer function of the movement of the L4Cs from excitation, and used this calculate what the piezo calibration must be, given that we now know all the other calibration factors in the system. In order to measure the transfer function, we connected the piezos to output channel 1 of CDS, which in our model is connected to the "SERVO" output. In diaggui, on the SERVO channel we turned on a white noise excitation between 0 and 100 Hz, with a large amplitude (1000). Then in MEDM, we opened the SERVO filter panel and turned on the output.

We measured the transfer function in diaggui (the CAL_OUT values for each L4C compared to the white noise excitation). We chose an area of the transfer function that was flat, which was at 30 Hz. The typical value of the transfer function in this area was about $30\times10^{-6}\left[\frac{\mu m}{V}\right]$. In the loop of the system (see Figure x), the part of the loop between the piezo and CDS (i.e. Platform → L4C → GEO preamp → AA → ADC → CDS) is accounted for by the filters we created earlier. So, to calculate the piezo calibration, we need only to consider the part of the loop between CDS and the piezo (i.e. CDS → DAC →AI → piezo). The AI component is just $1\left[\frac{V}{V}\right]$, so the transfer function can be written as:

$$TF\left[\frac{\mu m}{V}\right] = Piezo\left[\frac{m}{V}\right] \times DAC\left[\frac{V}{count}\right]$$

Substituting in the measured value of the transfer function and the calibration factor of the DAC:

$$Piezo\left[\frac{m}{V}\right] = 30 \times 10^{-12}\left[\frac{m}{V}\right] \times \frac{32768}{10}\left[\frac{V}{count}\right]$$

$$Piezo = 0.98 \times 10^{-7}\left[\frac{m}{V}\right]$$

This is fairly similar to the published value of 1.3×10^{-7} (a difference of $\tilde{2}8\%$).

3 Filters

The filters we developed to correct and control the system fall into three categories: Calibration Filters, Actuator Corrections, and System Controller. Within each of these categories, there are both frequency dependent filters and flat gains. I discuss in detail here the frequency dependent components.

3.1 Calibration Filters

The Calibration Filters primarily relate to the correction of the seismometer response. The first component of this filter is the inverse of the transfer function of the seismometer (ie the physical motion of the mass and spring system in the seismometer relative to the ground). To get the inverse of the transfer function, we first need to fit the non-inverted transfer function (see Figure 6). The fitting process is a delicate balance between closely matching the magnitude of the function, with a limited amount of phase loss.

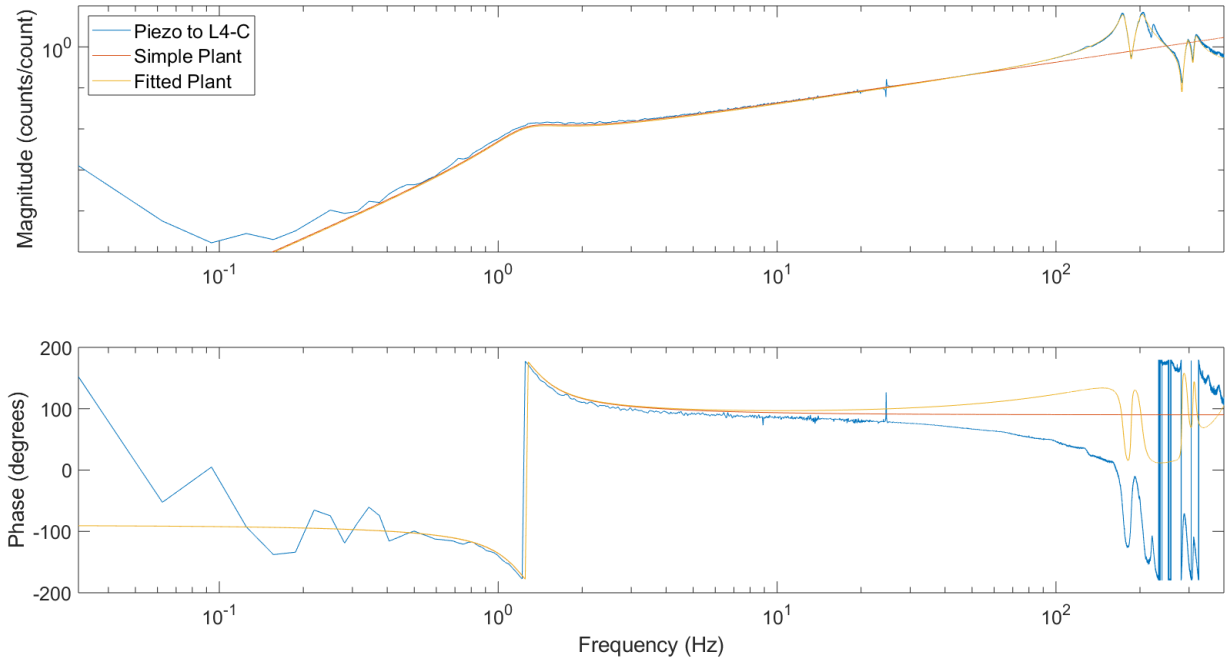

Figure 6: Fitting the transfer function of the seismometer response relative to the ground. The Simple Plant line is a model of the transfer function based only on the resonant frequency and Q of the geophone used to create the transfer function. The second fitted transfer function also fits the higher frequency oscillations.

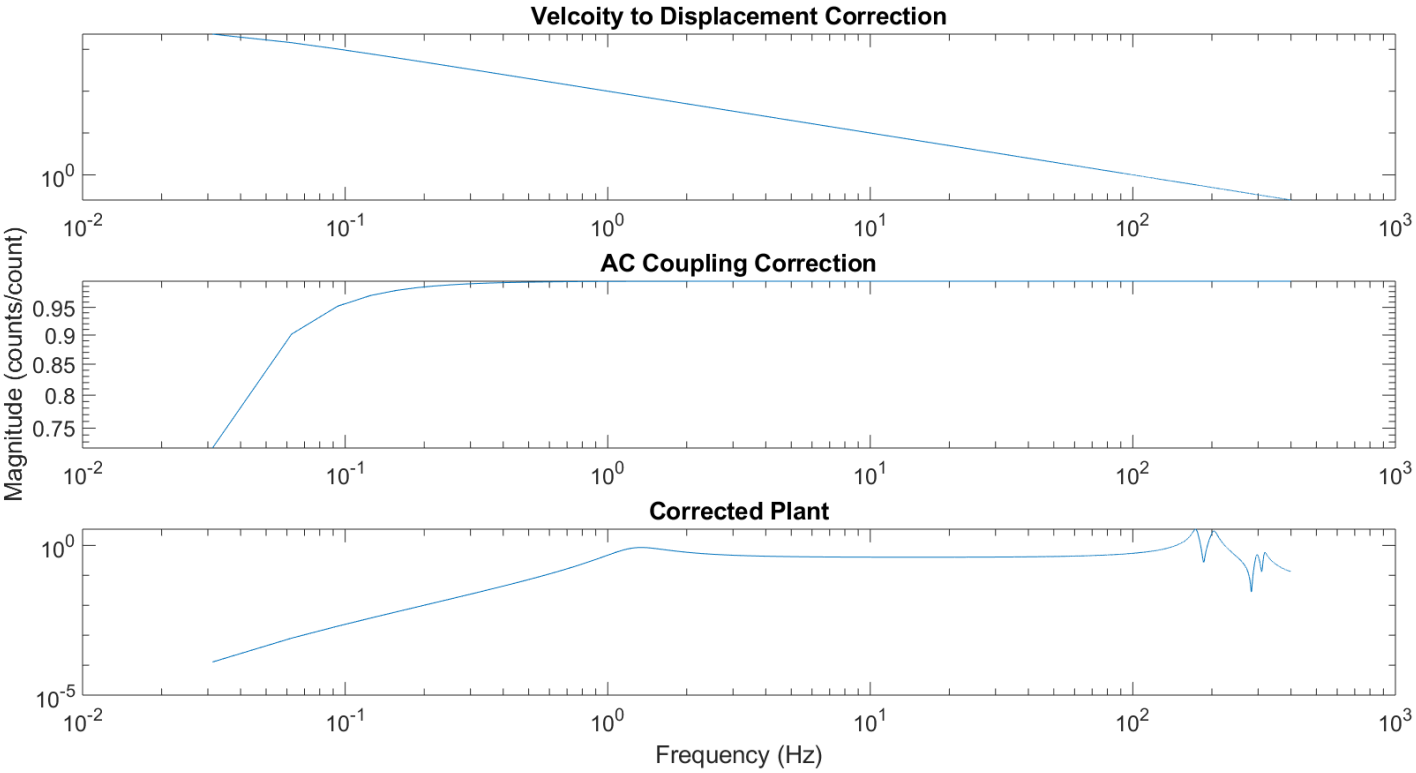

Figure 7: Corrections to the fitted plant inversion. Top: Velocity to displacement correction. Middle: Roll off at low frequencies to prevent infinite signal at 0 Hz. Bottom: The fitted transfer function from Figure 6 with these corrections applied.

The second component of the filter is the velocity to displacement response. The transfer function in just discussed is in terms of the *motion* of the seismometer, as in it measures in terms of $\left[\frac{Volts}{m/s}\right]$, and we need a function that is in $\left[\frac{Volts}{m}\right]$. The correction is quite simple - the conversion from velocity to displacement can be written as an integral of velocity over frequency, which results in $\frac{1}{f}$. This can be represented by a pole at 0 Hz; however, this is not physically possible, so the pole is actually placed at some low frequency, in this case 30 mHz. Additionally, this causes the response to go to infinity at 0 frequency. To avoid this, we simply add AC coupling at 30 mHz, which rolls off the signal between 0 and 30 mHz. These corrections are shown in Figure 8.

3.2 Actuator Corrections

The Actuator Correction filters are responsible for correcting the resonant motion and noise of the actuator platform. There are two components to this correction - low and high frequency. The low frequency component is fairly simple, as it is fit with the ringdown parameters discussed in Section 2.2.2. The high frequency component consists of different platform resonances and actuator noise, and is more difficult to fit. To start, we attempted

automatically fitting the function with a MATLAB function. However, this does not work particularly well, because the fit often includes right-hand-plane zeros. On their own, RHP zeros can be stable. However, we need to invert this function, which would make the RHP zeros into RHP poles, which are not stable. We also tried inverting the function and then automatically fitting, but the function was unsuccessful. As an alternative, we fit the function by hand. This fitted function can then be inverted and used as a filter. See Figure 8 for details.

3.3 System Controller

With all our filters in place, the system from the input to the output should now be ≈ 1 at middle frequencies, and roll off at low and high frequencies. We also added a boost to this, which amplifies the signal at the middle frequencies. To create this, we chose an upper Unity Gain Frequency (UGF) and a lower UGF. The upper UGF is based on how quickly we can control the platform, with limited phase loss. The lower UGF is chosen based on the point at which our piezos cannot move enough to cancel out the electronic noise of the system (ie at the point at which the "motion" of the noise is greater than the physical amount the piezos can actuate the platform).

4 Controlled System

Our controlled system is shown in Figure 9. For this controlled system, we used an L4C as the reference, and calculated our ground motion suppression based off of the L4C. This was a successful first attempt at an actively controlled platform. We got near to the noise floor of the L4C instrument. Later in the project, we increased the gain of the pre-amplifier by a factor of four, which should decrease all the measurements by a factor of four as well, bringing the measurement quite close to the noise floor at some frequencies.

While we were able to get an actively controlled platform with the L4C as the controller, the goal was to use the S-13 as the controller, as it has much better measurement capabilities. We designed and implemented a controller for the S-13. When we attempted to actively control the system, our controller was unstable. We later found, when we took a high resolution low frequency measurement, that the gain of the S-13 is much greater than expected at low frequencies (see Figure 10). We do not currently have a physical explanation for this phenomenon.

5 Conclusions

The majority of the time in this project was spent calibrating the 1D system components. With these calibrations, were able to successfully actively control the platform with an L4C, minimizing the ground motion seen by the geophones. However, we were unable to control the platform using the S-13, due to the aforementioned issues. A next step in this

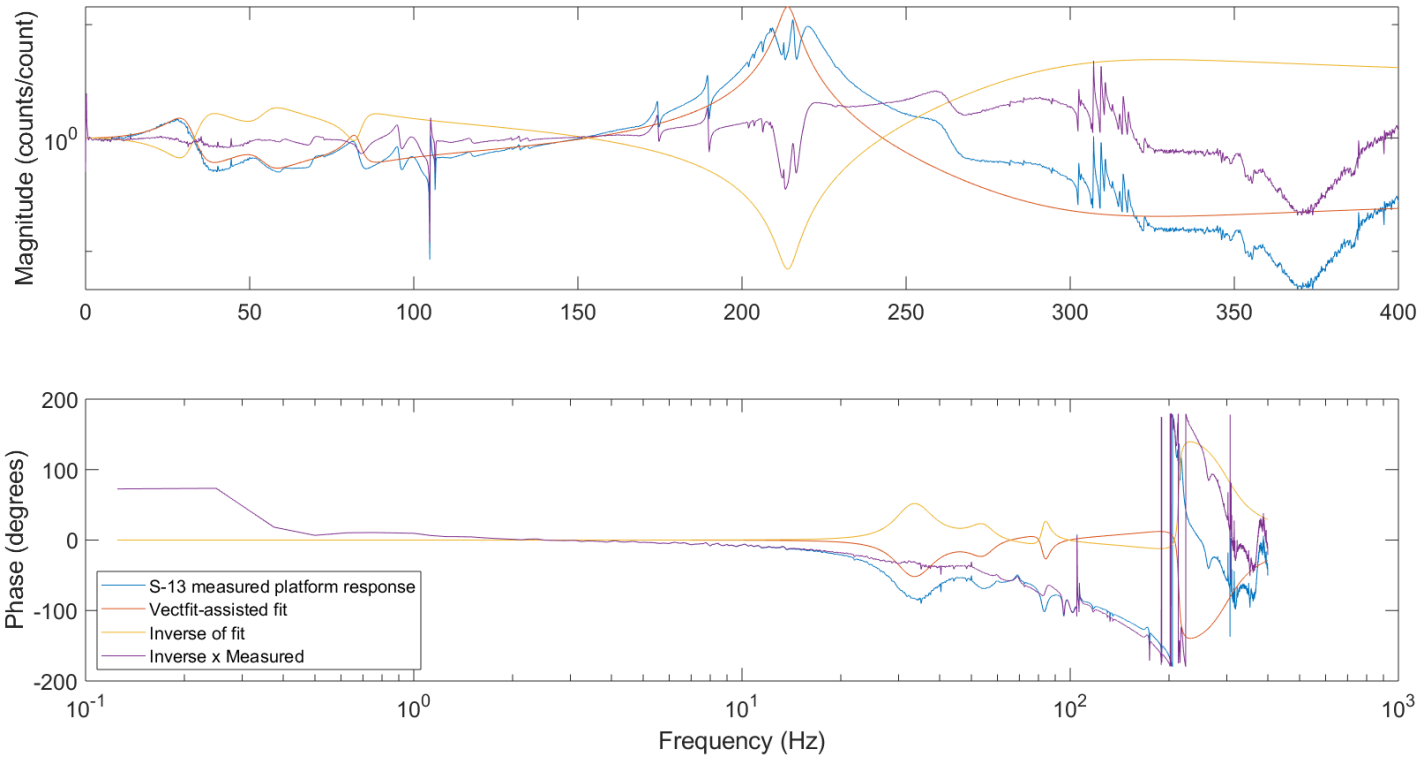

Figure 8: Creating Actuator Corrections. The first trace, "S-13 measured platform response," is the transfer function of the motion of the S-13 relative to the ground. This was measured with the Calibration filters applied. The second trace, "Vectfit-assisted fit," shows the fit we created for the transfer function, and the "Inverse of fit" trace is simply this fit inverted. The final trace, "Inverse x Measured," shows the measurement in trace 1 multiplied by the inverse fit shown in trace 3. The result of this is what we expect to see when we measure the system with the Actuator Corrections also applied. Notice that in this trace, the value is ≈ 1 and fairly flat, except where we were unable to closely fit the peaks of the original measurement.

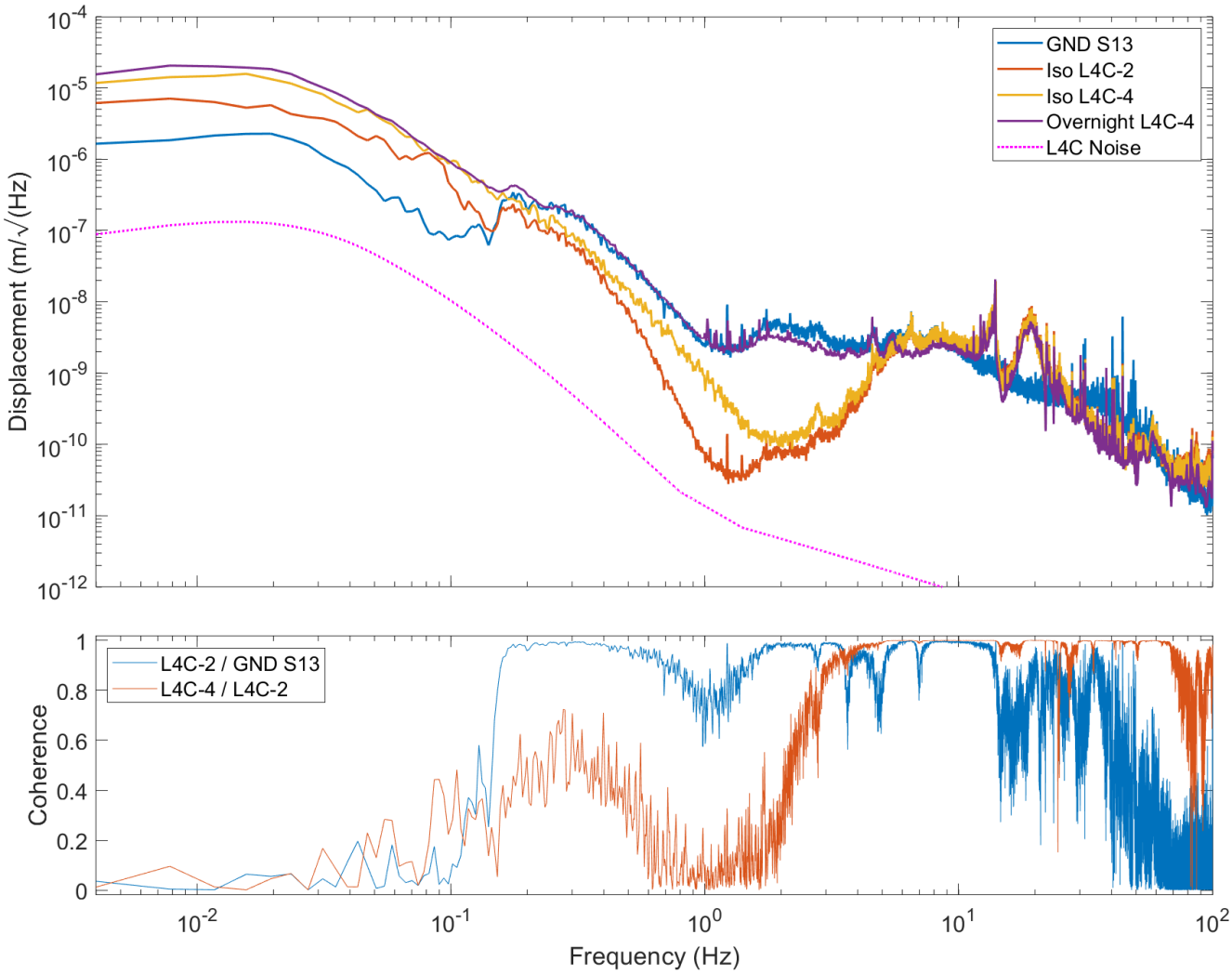

Figure 9: Spectrum and Coherence of the controlled system, using an L4C as the reference for active control.

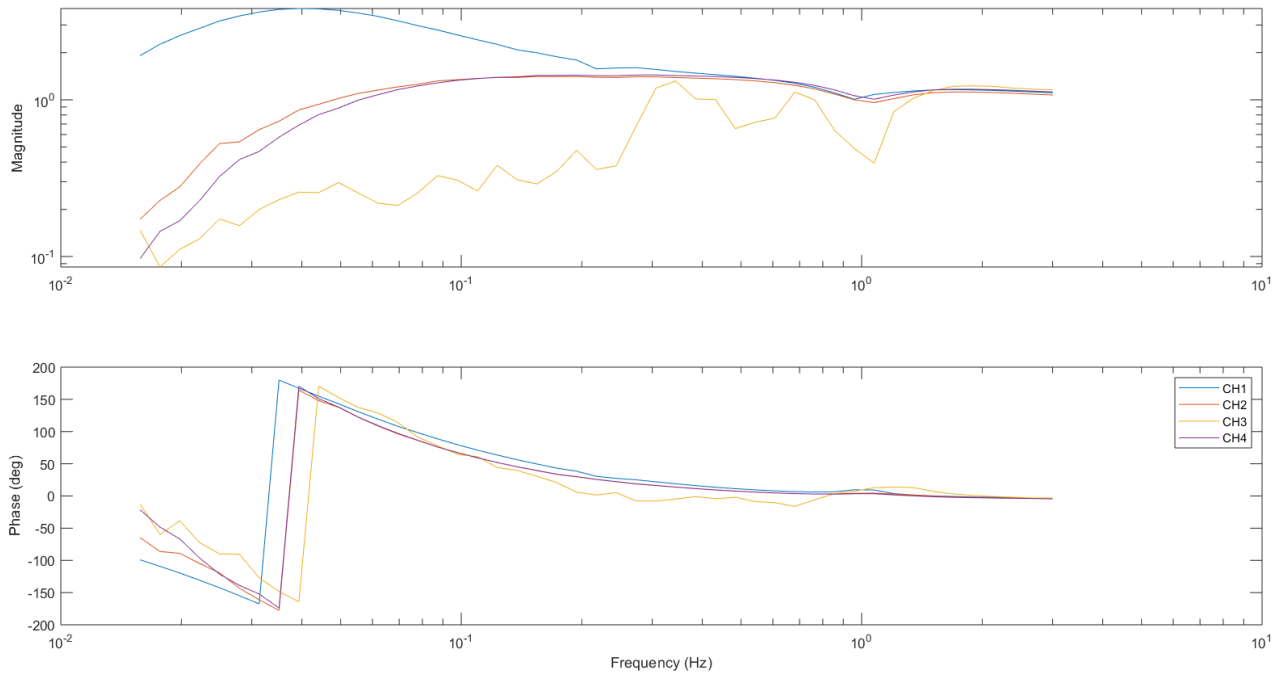

Figure 10: S-13 Response at low frequencies. Notice how much greater the magnitude of the S-13 trace is at low frequencies than the L4C traces. This is unexpected, and we do not yet understand why this happens.

project would be determining the cause of the high gain in the S-13, so it can be used as a better reference for the controller.

5.1 Future Work

In the future, there are two main components to work on.

1. Create a noise budget for the system; and
2. Incorporate the Homodyne Quadrature Interferometer (HoQI) into the system. The HoQI is the instrument that will eventually be used in the 6D system. This summer, I assembled two HoQIs (detailed in Appendix A), but was not able to connect them into the system. Adding the HoQI will:
    - Allow for a better measurement of the ground motion through the interferometer, which leads to better active control.
    - Lead to a better measurement of the noise floor of the 1D system.

Acknowledgments

Thank you to Conor Mow-Lowry for his mentorship on this project. Thank you as well to Sam Cooper and Leo Prokhorov for their guidance in the lab. And of course, thank you to the University of Florida for this opportunity, and the University of Birmingham for hosting me.

References

[1] A. Einstein, "Über Gravitationswellen (German) [On Gravitational Waves]," *Königlich Preußische Akademie der Wissenschaften*, p. 154–167, Feb 1918.

[2] B. P. Abbott, et al., "Observation of Gravitational Waves from a Binary Black Hole Merger," *Phys. Rev. Lett.*, vol. 116, p. 061102, Feb 2016.

[3] H. Yu, D. Martynov, S. Vitale, M. Evans, D. Shoemaker, B. Barr, G. Hammond, S. Hild, J. Hough, S. Huttner, and et al., "Prospects for Detecting Gravitational Waves at 5 Hz with Ground-Based Detectors," *Physical Review Letters*, vol. 120, no. 14, 2018.

[4] C. Mow-Lowry and D. Martynov, "A 6D Interferometric Inertial Isolation System," Feb 2019.

A HoQI Assembly

This appendix details the assembly instructions for the prototype of the Homodyne Quadrature Interferometer (HoQI).

1. Place all components on the board (shown in Figure 11) to make sure everything fits properly, and to confirm the orientations of the components (especially the polarizing beamsplitters – see Figure 12).

Figure 11: The base of the HoQI with no components attached.

2. Glue down the polarizing and non-polarizing beamsplitters and diagonal mirror with a small amount of superglue (shown in Figure 13). Make sure components are straight by pressing them against the two ridges on the base.

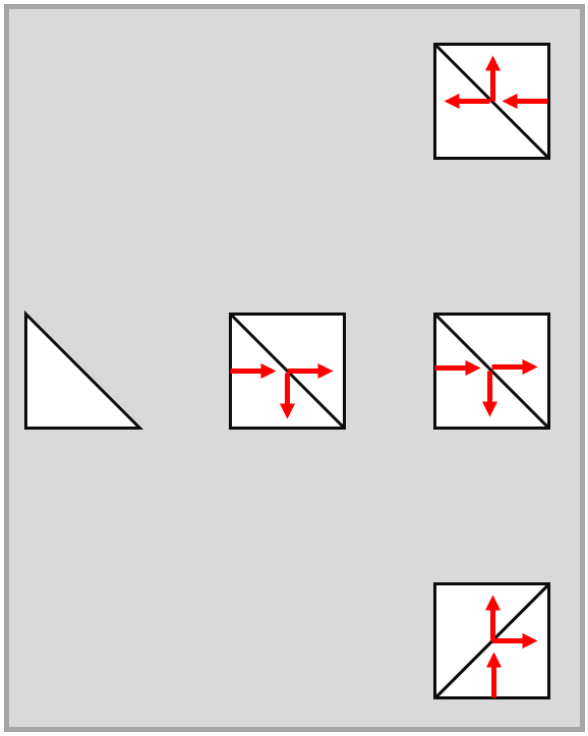

Figure 12: The orientation of beamsplitters on the base.

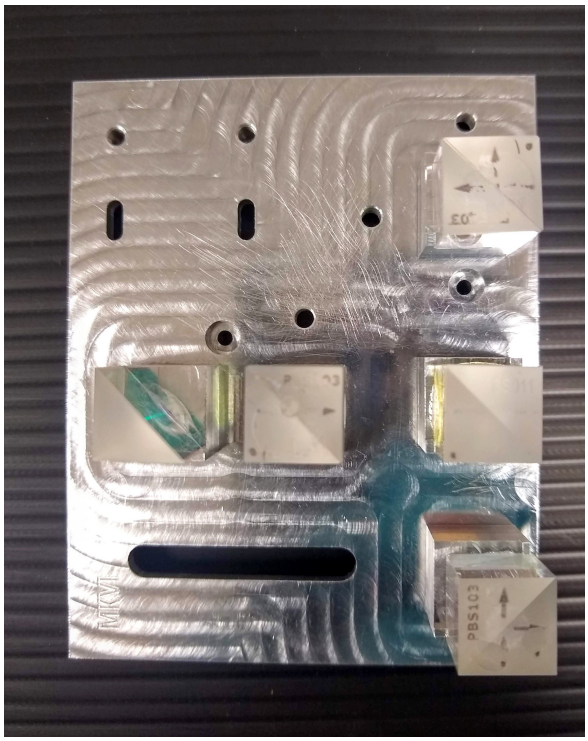

Figure 13: The HoQI with the beamsplitters and diagonal mirror attached.

3. On the waveplate holder, attach the lip to both sides to help secure the waveplates (see Figure 14). Place waveplates in waveplate holder at 45°relative to the horizontal.

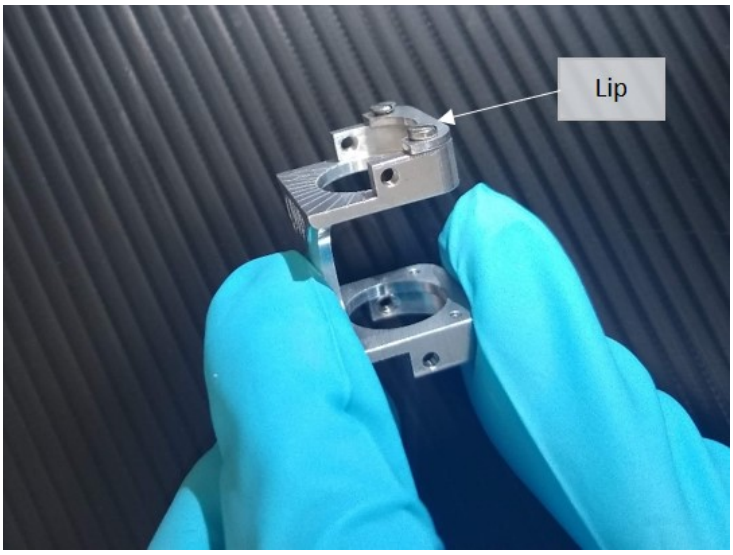

Figure 14: Attaching the lip to the waveplate holder.

4. Glue the waveplate holder to the non-polarizing beamsplitter, with the half waveplate (HWP) orientated closer to where the test mirror will be, and the quarter waveplate (QWP) towards the top of the HoQI. Note that the waveplate holder should be placed off center, so that the QWP is closer to the beamsplitter. This is to allow for access to a screw later. See Figure 15 for details.

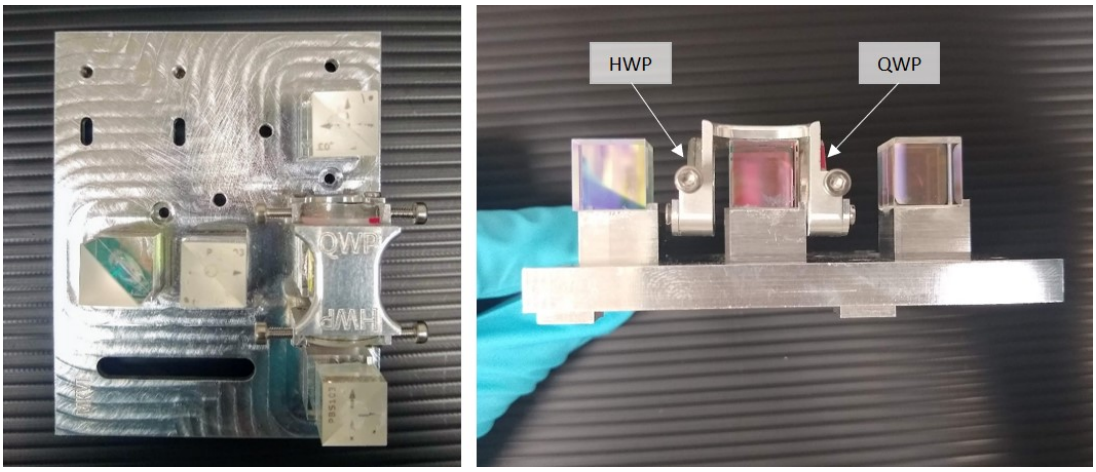

Figure 15: (left) The orientation of the waveplates. (right) The waveplates should be placed off center.

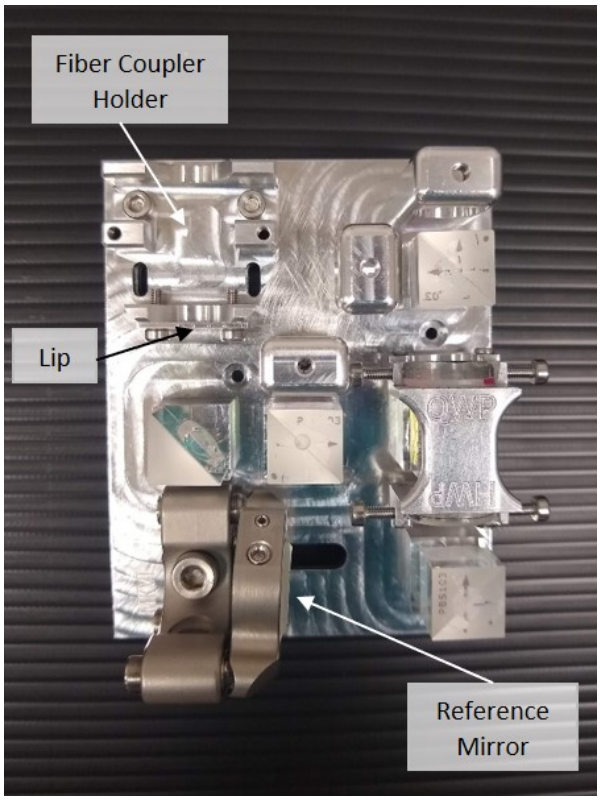

Figure 16: Attaching the Reference Mirror and Fiber Coupler Holder.

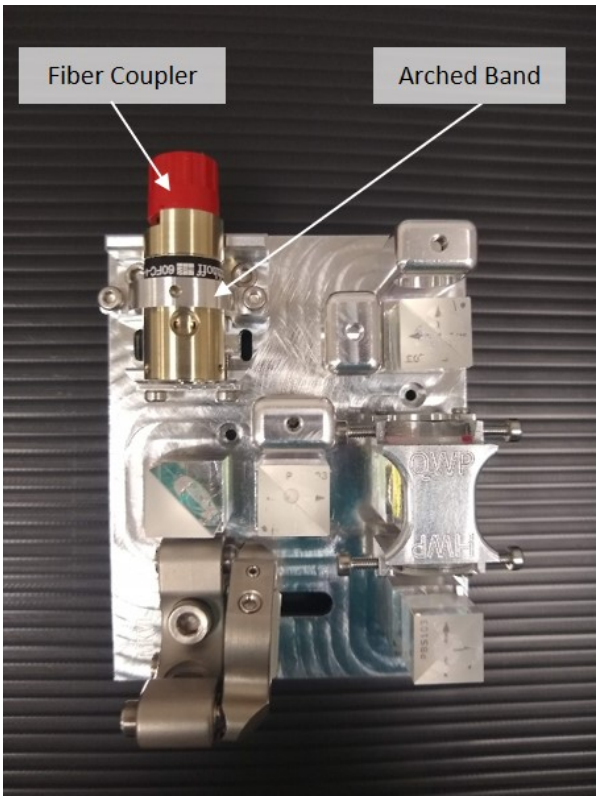

Figure 17: Securing the Fiber Coupler to the HoQI.

5. Place reference mirror in the reference mirror holder, and screw the holder to the base (see Figure 16). The location of the holder along the slot is designed to be adjusted throughout the process.

6. On the fiber coupler holder, screw on the lip to prevent the fiber coupler from sliding forward. Attach the fiber coupler to the base (Figure 16). Attach fiber coupler to the fiber coupler holder with the arched band (Figure 17).

7. Gently invert the L4C. Loosely attach the HoQI to the L4C at the three connection points. Invert the L4C and check that the mass is still free to move. Tighten screws as much as possible while still allowing the mass to move freely. If you find that the screws are too long to be tightened properly and no shorter ones are available, use a spacer to effectively shorten the screw as needed.

8. Insert the test mirror into the test mirror holder. In this iteration, the holder was too small, and we had to use a Dremel to widen the holder. If this is necessary, make sure to do it evenly and very gradually.

9. The final step is to attach the test mirror to the mass. Invert the L4C (so that the mass is not moving). Place a photodiode holder on the HoQI. This is to stabilize the test mass as it is attached. Without any glue, place the test mirror on the photodiode holder, and check to make sure it sits level, is centered above the polarizing beam splitter, and is flush to the mass. Now, add glue and gently attach the test mirror to the mass.

10. Let the glue set for at least ten minutes. It may take a few tries for the test mirror to stick. If it does not stick, clean off any glue using acetone and then isopropyl alcohol. Be especially careful when cleaning the mass, as it is very fragile in that direction. When the mirror is thoroughly stuck to the mass, carefully invert the L4C. Make sure to hold onto to the photodiode holder while inverting so that it does not fall.